Wire-Like Tip-To-Tip Linked Assemblies of CdSe-CdS Quantum Rods Promoted on Supramolecular Nanofibers of Hybrid Organo- and Hydrogels

Arkajyoti Chakrabarty, Mitasree Maity, Guillaume Raffy, Samuel Marre, Cyril Aymonier, Uday Maitra, André del Guerzo

ACES Asian Chemical Editorial Society

DOI: 10.1002/cnma.201900428

CHEMNANOMAT
Full Paper

Wire-Like Tip-To-Tip Linked Assemblies of CdSe-CdS Quantum Rods Promoted on Supramolecular Nanofibers of Hybrid Organo- and Hydrogels

Arkajyoti Chakrabarty,*[a, b, c] Mitasree Maity,[a, b] Guillaume Raffy,[a] Samuel Marre,[c] Cyril Aymonier,[c] Uday Maitra,[b] and André Del Guerzo*[a]

Abstract: A variety of core-shell CdSe-CdS nanorods or quantum rods (QRs), both sphere (CdSe) in rod (CdS) and rod (CdSe) in rod (CdS) have been synthesized in a seeded-growth approach using a very efficient and highly thermally stable steroidal cadmium precursor replacing the more common CdO: cadmium deoxycholate. The core-shell QRs display high photoluminescence quantum yields (40–75%) and high molar absorption co-efficient ($\epsilon = 10^6\ M^{-1}\,cm^{-1}$). Sphere-in-rods QRs can be co-assembled with the organogelator diethylaminolithocholyl iodide in 1,2-dichlorobenzene and with the hydrogelator calcium cholate in water to form hybrid gels. These organic-inorganic hybrid soft materials are translucent and brightly red-luminescent. The nanofibers composing the gel network act as a scaffold to support the dispersed QRs and impede their self-aggregation. Furthermore, formation of original wire-like assemblies of the nanorods is promoted in these gels, in particular in the hydrogel. This orientation occurs by a QR tip-to-tip interaction and is proposed to be driven by the amphiphilic behaviour of the QRs: laterally capped by negatively charged TGA (thioglycolic acid) ligands and un-capped on the tips due to TGA unbinding. The combination of nanofiber-forming hydrogelators and elongated quantum rods is promising in the perspective to form hybrid nanostructures with anisotropic optic or electronic properties.

1. Introduction

During the last few decades, there has been an enormous interest in the controlled synthesis of semiconductor nanocrystals (NCs) with tailored shapes, compositions and properties.[1–5] Moreover, self-assembly of these NCs with anisotropic shapes has drawn attention to mimic systems such as protein assemblies, templated by DNA and peptides, leading to robust nanostructures with collective and improved properties.[6–8] These NC-assemblies, especially the 1D-assemblies can be very good candidates for directional carrier transport and energy transfer.[9]

Among the anisotropic NCs, a particularly important family is the semiconductor nanorods or quantum rods (QRs) which exhibit linearly polarized emission with high photo-stability depending on their shape, structure and topographical orientation.[10–13] Seeded core-shell QRs such as CdSe-CdS QRs containing a spherical seed embedded in an elongated shell (sphere in rod, S-in-R) or a rod seed in an elongated shell (rod in rod, R-in-R), display high quantum efficiencies of emission due to the efficient overlap of electron and hole wave functions yielding high radiative rate constants, and passivating shells reducing the non-radiative decay due to trapping of excitons in surface defects.[14–16] Moreover, the luminescence is highly linearly polarized along their long axes because of the quasi-cylindrical symmetry of the CdS shell and the resulting crystal field effect on the radiative charge recombination within the rod.[17] Colloidal syntheses of CdSe-CdS QRs, very well-known to material chemists, involve using mainly cadmium oxide as Cd-precursor and phosphonic acid ligands suitable for anisotropic growth at high temperatures ($>300\,^{\circ}C$) and their optical, electronic and structural properties have been subjected to extensive studies for the last two decades.[18–23]

Self-assembly of CdSe-CdS QRs is controlled by modulation of interparticle interactions and interfacial energy in the presence of external fields, binary solvent-nonsolvent mixtures and solid/liquid/air interfaces.[24–27] Interestingly, there are quite a few reports in literature of extensive interconnections between NC building blocks leading to the 3D self-assembly and formation of "gels" and "aerogels," where a marriage of nanoscale properties with macroscale world takes place.[28–32] These aerogels are low-density porous materials with large open pores (<2 nm or 2–50 nm sizes) and high inner surface areas and are formed by self-aggregation followed by CO_2 supercritical drying.[33,34] In this regard, 1D-QRs are attractive variety of NCs as their high aspect ratios are beneficial for extensive interconnection leading to anisotropic assemblies and aid "gel" formation.[35–38] Thus, by carefully choosing the molecular interactions at the QR interfaces, self-assembly of QRs has been triggered either via straightforward intermolecular

[a] Dr. A. Chakrabarty, Dr. M. Maity, G. Raffy, Prof. A. Del Guerzo
Univ. Bordeaux, CNRS, Bordeaux INP, Institut des Sciences Moléculaires, UMR 5255, 351 Cours de la Libération, 33400 Talence, France
E-mail: arkajyoti.chakrabarty@gmail.com
andre.del-guerzo@u-bordeaux.fr

[b] Dr. A. Chakrabarty, Dr. M. Maity, Prof. U. Maitra
Department of Organic Chemistry
Indian Institute of Science
Bangalore-560012, India

[c] Dr. A. Chakrabarty, Dr. S. Marre, Dr. C. Aymonier
CNRS, Univ. Bordeaux, Bordeaux ICMCB, UMR 5026, F-33600, Pessac, France

Supporting information for this article is available on the WWW under https://doi.org/10.1002/cnma.201900428

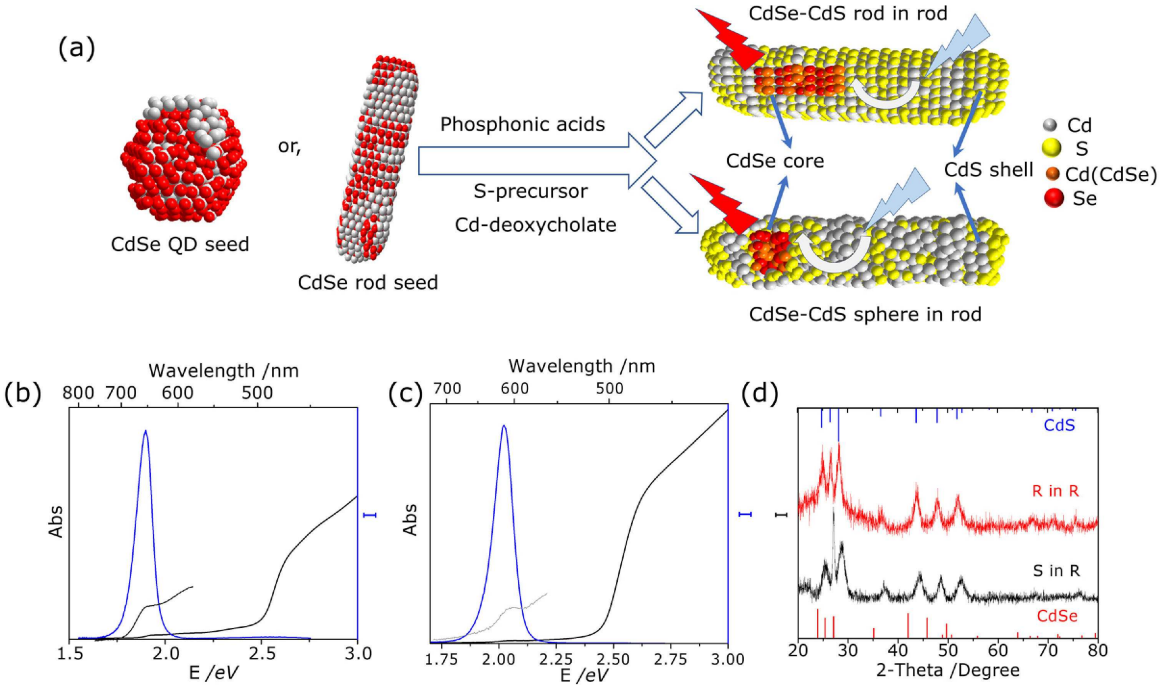

Figure 1. (a) Schematic of seeded-growth synthesis of core-shell CdSe-CdS QRs (S-in-R and R-in-R); (b) absorption (black) and photoluminescence (PL, blue) spectra of 53 nm long CdSe-CdS QRs, R-in-R (excitation wavelength = 425 nm), zoomed CdSe peak is shown as a black spectrum ; (c) absorption (black) and photoluminescence (PL, blue) spectra of 65 nm long CdSe-CdS QRs, S-in-R (excitation wavelength = 425 nm), zoomed CdSe peak is shown as a grey spectrum; (d) X-ray powder diffraction patterns of QRs (S-in-R, black and R-in-R, red). The stick patterns show standard peak positions of bulk wurtzite CdSe (bottom red sticks) and CdS (top blue sticks).

interactions between the capping agents or with the aid of predefined templates in presence of external stimuli such as temperature, solvent polarity, redox capacity or electromagnetic radiation (*e.g.* light).[39–43] Although there are reports on self-assembly of QRs driven by interparticle forces, the potential of ordering the assembly of QRs on supramolecular gel fibers has still to be fully explored and exploited. In a recent report, we have shown the alignment of CdSe-CdS QRs on organogel nanofibers due to the interactions of the QRs with the nanostructured fibers of a polyaromatic organogelator (2,3-didecyloxyanthracene, DDOA) in DMSO.[44] Thus, in that case, interparticle interactions were not at the origin of the organization.

In this work, the organogelation and hydrogelation properties of bile acid derivatives was exploited. Bile acids/salts are physiologically important amphiphilic detergents having a hydrophobic rigid steroidal backbone (convex β-face) and hydrophilic hydroxyl groups (concave α-face), which are the characteristics of the coprostane class of steroids.[45–47] Although bile acid based hydrogelators are well-known and more abundant, the organogelators are relatively rare.[48–57] The organogelation properties of the bile acids arise from the van der Waals forces and intermolecular hydrogen-bonding interactions involving the hydroxyl groups, whereas the hydrogelation properties arise from mainly hydrophobic interactions. It was previously reported that a lithocholic acid derived quaternary ammonium iodide salt forms organogels in various organic solvents.[58] The gelator diethylaminolithocholyl iodide (DEALI) was chosen to form a hybrid material with the trioctylphosphine oxide (TOPO)-capped QRs CdSe-CdS QRs (S-in-R) as both gelator and QRs are soluble/dispersible within the same solvent, 1,2-dichlorobenzene (DCB). Additionally, the properties of a hybrid hydrogel were studied using sodium cholate and calcium nitrate in water,[54] which form a gel upon mixing warm solutions of both components, to which the thioglycolic acid (TGA) capped CdSe-CdS QRs (S-in-R) were added. The QRs prepared herein were obtained with an original precursor, cadmium deoxycholate ($Cd(DCh)_2$), instead of the more common CdO precursor. Indeed, Cd-deoxycholate is thermally very stable and has been shown to allow the use of high temperatures (> 300 °C) for the synthesis of high quality CdSe quantum dots.[59]

2. Results and Discussion

2.1. CdSe-CdS Quantum Rods (S-in-R and R-in-R)

The core-shell CdSe-CdS QRs (S-in-R or R-in-R) were synthesized in two steps (Figure 1a). At first, 3 nm wurtzite spherical CdSe cores or 12 nm long CdSe rods were prepared using the highly thermally stable steroidal precursor cadmium deoxycholate ($Cd(DCh)_2$) instead of the most common CdO or cadmium carboxylate salts.[44,59,60] The use of this Cd-salt of deoxycholic acid as the precursor for the QR synthesis allows to explore a larger temperature range for the synthesis of nanocrystals and is additionally composed of an innocuous chemically inert

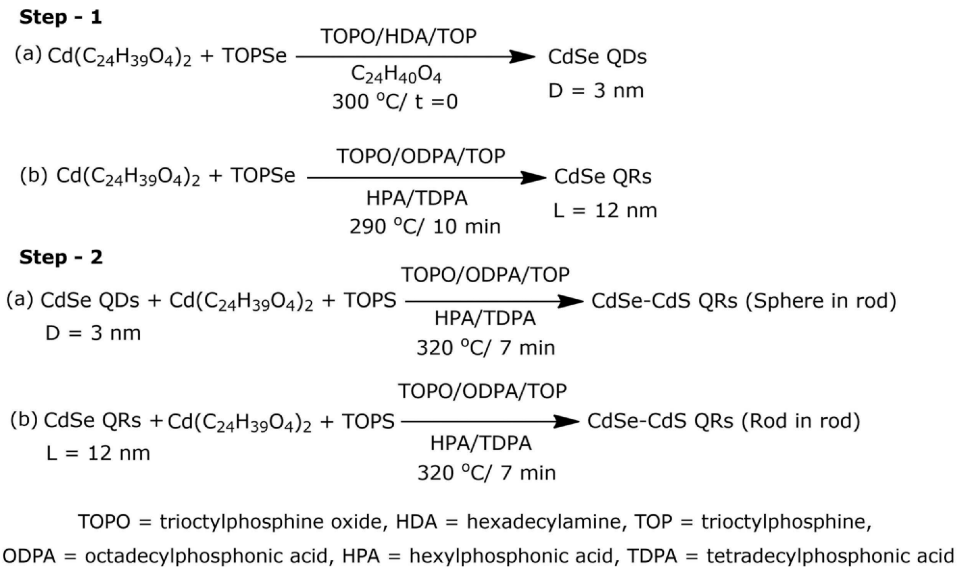

Scheme 1. Chemical transformations showing the formation of CdSe-CdS QRs (S-in-R and R-in-R) from cadmium deoxycholate (reactions are not balanced).

steroidal component. In the second step, a CdS shell of the QRs was grown by injection based "seeded growth" on the spherical or rod-shaped CdSe core with $Cd(DCh)_2$ and a solvent/ligand combination suitable for anisotropic growth. For the QRs (S-in-R) with large aspect ratio (AR = 9), a well-resolved peak at higher energy was observed along with the low-energy peak in the optical absorption spectrum (Figure 1c). The addition of the shell turns the green emission of the core to red in the core-shell QR (λ_{em} = 613 nm, Figure 1c for S-in-R, λ_{em} = 654 nm for R-in-R, Figure 1b). The emission of the core-shell S-in-R CdSe-CdS QRs is spectrally sharp, with a full-width-at-half-maximum (FWHM) of 27 nm, Stokes-shifted by only 37 meV. In contrast, in the case of R-in-R CdSe-CdS QRs the absorption has a featureless nature with a large onset in the higher energy region, along with a low energy peak (Figure 1b). The global Stokes shift[10] is 45 meV for the low aspect ratio R-in-R QRs (AR = 5), thus quite small and indicating a small dispersion in size. The FWHM of these QRs were 101 meV (35 nm). The QRs (S-in-R and R-in-R) show high photoluminescence quantum yields of 40–75% when excited at 527 nm and similar quantum yields were conserved after washing three times with a non-solvent. The quantum yields reported in literature for CdSe-CdS QRs influenced by the aspect ratios of the QRs, are ~70% (S-in-R) by Carbone *et al.*,[15] ~80% (S-in-R) by Talapin *et al.*,[16] 42–65% (S-in-R) and 36–76% (R-in-R) by Sitt *et al.*[17] However, the quantum yields were further improved to unity by introducing a second shell of CdS on CdSe-CdS QRs by "slow-injection growth" as described by Coropceanu *et al.*[14] Thus, the high quantum yields observed for our CdSe-CdS QRs signify the efficiency of synthesis method using cadmium deoxycholate as Cd-precursor. The CdSe-CdS QRs (S-in-R and R-in-R) are also bright, since extinction coefficients of $>10^6\ M^{-1}cm^{-1}$ are reached in the visible and near-UV ($5.1\times10^6\ M^{-1}cm^{-1}$ at 375 nm, $2.1\times10^6\ M^{-1}cm^{-1}$ at 473 nm). The spectral characteristics show that there is no graded shell formation due to alloying of the CdS shell with the CdSe seeds which would have led to a blue shift of the spectra of the alloy rods as compared to the seeds.[61] The XRD patterns of CdSe- CdS QRs (S-in-R and R-in-R) corresponds to the patterns of bulk CdS wurtzite (JCPDS no. 41-1049), since the weight of CdSe is almost negligible (< 0.5%) in the seeded rods (Figure 1d). The high intensity peak at 27.0° in the XRD pattern of S-in-R QRs indicates that the growth occurs along the (002) plane. However, scattering from amorphous material at low angles (~22.0°) was visible in both the XRD patterns and might be due to residual organic ligands attached to QR surfaces. The chemical transformations leading to the formation of CdSe-CdS QRs from Cd-deoxycholate is shown in Scheme 1.

The high crystallinity and homogeneity in shapes of CdSe-CdS QRs (S-in-R and R-in-R) are further confirmed by TEM images, in which the formation of highly organized 2D-assemblies of QRs with nematic or smectic ordering is observed (Figure 2a, c). The slight asymmetry in the rods also indicates that the seed is on one side of the QR, and not in the center. TEM images of R-in-R QRs revealed that the tendency of the QRs to self-assemble among themselves due to depletion attraction forces.[24,25] HRTEM image of 53 nm long R-in-R QRs (Figure 2b) and 65 nm long S-in-R QRs (Figure 2d) further show little occurrence of stacking faults over the entire structure with lattice spacing of 3.37 Å corresponding to (002) plane of CdS wurtzite phase and 3.54 Å corresponding to (002) plane of CdSe wurtzite phase, which is in good agreement with XRD patterns in Figure 1d. The histograms of shape distribution (length and diameters) of the homogenously shaped QRs (R-in-R) in Figure 2a have L = 53.2 ± 6 nm and D = 10.4 ± 2 nm with AR = 5 (Figure S3a–b). On the other hand, QRs (S-in-R) in Figure 2c shows that the 65 nm long and 7 nm thin QRs have distributions of length and diameters of 4 and 1 nm respectively (Figure S3c–d). The R-in-R QRs were significantly thicker in comparison to S-in-R indicating incorporation of rod seeds.

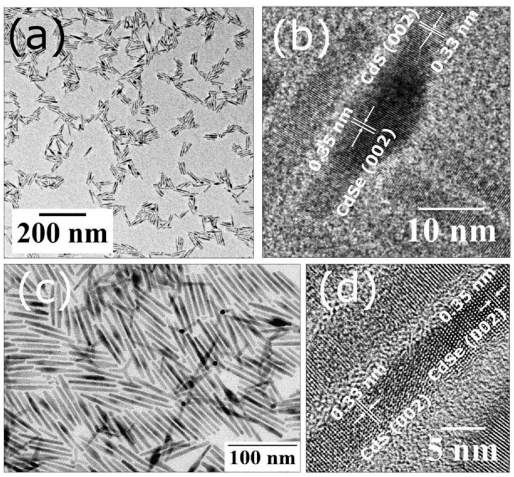

Figure 2. Transmission electron microscopy images of CdSe-CdS QRs and their average rod D (measured at the center of the QR) and L: (a) (R-in-R) (10.4 ± 2) nm and (53.2 ± 6) nm, AR = 5; (b) HRTEM image of 53 nm long QRs (R-in-R) showing little occurrence of stacking fault over the entire structure with lattice spacing corresponding to (002) planes. (c) (S-in-R) (7.3 ± 1) nm and (65 ± 4) nm, AR = 10 showing 2D-smectic phases; (d) HRTEM image of 65 nm long QRs (S-in-R) showing high crystallinity with (002) planes.

Increasing the concentration of seeds of QDs during synthesis resulted into QRs (S-in-R) with shorter lengths (20 ± 1 nm) and diameters (5.7 ± 1 nm, Figure 4a and **S4**). Thus, the high quality CdSe-CdS QRs (S-in-R or R-in-R) synthesized using a highly thermally stable cadmium precursor, $Cd(DCh)_2$ have superior optical properties, long-term photostability and high crystallinity and have optical properties comparable to those found in literature.[15–17]

2.2. Hybrid Material of CdSe-CdS QRs (S-in-R) and Diethylaminolithocholyl Iodide (DEALI) Organogel in DCB

S-in-R QRs having high PL QY (40–75%) and sharp emission were dispersed within the self-assembled fibrillar network (SAFIN) of the diethylaminolithocholyl iodide (DEALI, Figure S1 in supporting information) organogel in 1,2-dichlorobenzene (DCB). This solvent was chosen since the TOPO-capped CdSe-CdS (S-in-R) 20 nm long QRs were highly dispersible within, coinciding with the fact that DCB can be gelled by DEALI. A high concentration of CdSe-CdS QRs (S-in-R, 500 nM) was dispersed in a 20 mM DEALI gel in DCB (Figure 3a) and yielded a golden-brown colored translucent gel (Figure 3b, left). Hitherto, the non-luminescent DEALI organogel in DCB turned into a bright red emitting organogel under UV illumination (Figure 3b, right). As compared to a dispersion of CdSe-CdS QRs in DCB (at same concentrations), the hybrid gel showed a lower emission intensity with the same emission maximum (λ_{em} = 617 nm, Figure S5a). The quenching may be attributed to the iodide ions present in gelator, although the exact mechanism could not be determined. The absorption and excitation spectra of the hybrid gel were similar, indicating that the energy transfer from shell to core is very efficient in the QRs embedded in the gel (Figure 3a). The thermal and mechanical stability of gel-QR hybrid material can offer insight on the presence of interactions between gel nanofibers and the added quantum rods. Hence, rheological and thermal stability studies of the

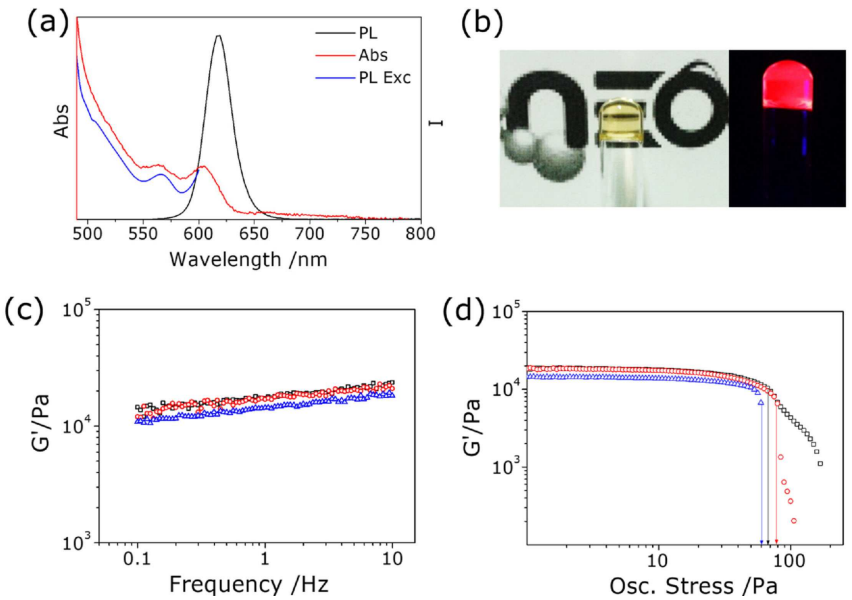

Figure 3. (a) Overlay of PL (excitation wavelength = 425 nm), PL excitation (λ_{em} = 617 nm) and absorbance of CdSe-CdS QRs (S-in-R)-DEALI hybrid gel; (b) photograph of the hybrid gel under visible light and UV-excitation (λ_{ex} = 365 nm); (c) frequency sweep test with a fixed oscillatory stress of 1 Pa (black squares: 20 mM DEALI pristine organogel in DCB, red circles: 20 mM organogel/50 nM QRs, blue triangles: 20 mM organogel/ 500 nM QRs; (d) oscillatory stress sweep test with a fixed frequency of 1 Hz showing the breaking point of the hybrid gel with different concentrations of the QRs of the same samples with same symbols.

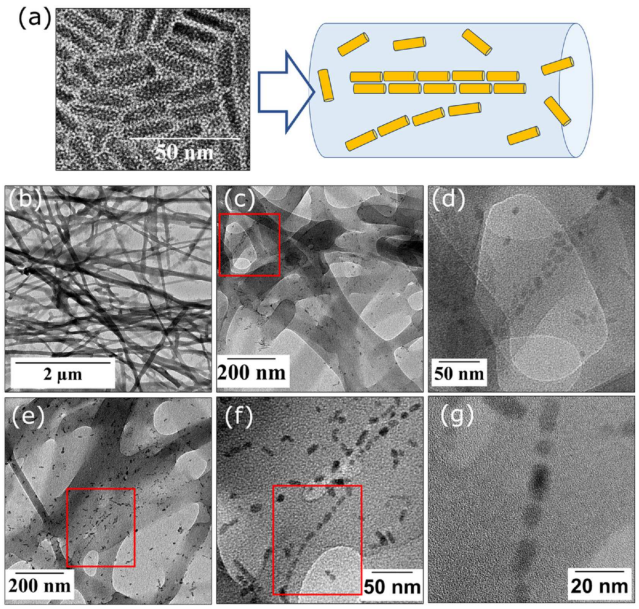

Figure 4. (a) TEM image of 20 nm long QRs and schematic representation of supramolecular co-assembly of QRs and NFs; (b) TEM image of 500 nM CdSe-CdS QRs (S-in-R) in 20 mM DEALI hybrid gel in DCB: the entire gel network showing entangled fibers with cross-fibrillar zones; (c–d) zoomed-in images of the rectangular box showing ordered assemblies of QRs in line with each other; (e–g) another region in the material zoomed in with similar assembled QRs in linear arrays.

hybrid gels were performed at different concentrations of QRs (50 and 500 nM, respectively). The thermal stability of the CdSe-CdS QRs-DEALI hybrid organogel in DCB was measured in the conventional "inverted test-tube method" and the gel-melting temperatures are gathered in Table 1.

The pristine DEALI gel in DCB melts at 77 °C, whereas improvement of thermal stability of the hybrid gel by six degrees (83 °C) is observed with the lower doping with QRs (50 nM). However, with further increase of the QRs concentration to 500 nM, the thermal stability of the hybrid gel is limited to 80 °C. These results indicate that a small amount of QRs stabilizes the hybrid material, whereas the stability can be affected with larger amounts of QRs. Similar stabilization effects have been observed previously in hybrid organogels.[44] In order to ascertain that the stabilization was not due to free capping agents remaining from the synthesis of QRs, repeated washing procedures of the QRs were performed in order limit the presence of capping agents to $<5\%$ wt (ligand/QR, QRs being at most 10^{-3} %mol as compared to DEALI). However, the capping agents attached at the surface of the QRs could interact favourably with the gelator molecules through their long lipophilic alkyl chains as this renders the QRs soluble in a non-polar aromatic solvent (DCB). Furthermore, presence of deoxycholic acid along with TOPO on the surface of the QRs is evident in the FT-IR spectrum of the QRs (Figure S6) and this yields more support to the co-assembly due to the structural similarity between the capping ligand and the gelator.[62–65]

Table 1. Thermal stability and rheological parameters of the CdSe-CdS QRs-DEALI hybrid organogel in DCB.

Organogel/QRs (mM/nM)	T-gel (°C)	G' (Pa)	G'/G''	σ* (Pa)
20 mM/0 nM	77	17330	7	66
20 mM/50 nM	83	17000	5	80
20 mM/500 nM	80	14400	6	59

In order to obtain further evidence of the interaction of QRs with the nanofibers, rheology was performed to determine the mechanical properties of the hybrid gels. Gels are visco-elastic soft-solids as they both store and dissipate energy.[66,67] Dynamic rheological experiments (frequency sweep test at a fixed oscillatory stress of 1 Pa and stress sweep test at a fixed frequency of 1 Hz) are shown in Figure 3c–d. In Table 1, the significant rheological parameters such as storage (G') and loss moduli (G''), stiffness (G'/G'') and yield stress (σ*) of the pristine DEALI and hybrid gels are described. The pristine gel showed high mechanical strength with G' in the order of 17 kPa. Upon doping of QRs, the hybrid gels kept similar G' values (14–17 kPa) and thus stiffness. This confirms that QRs did not have any adverse effect on the 3D network of fibers consisting of flocs with robust junction zones.[68,69] The yield stress, indicating the mechanical stability of the hybrid gels, is slightly higher upon lower doping with QRs (50 nM) as compared to the pristine gel and decreases with the highest doping of QRs (500 nM). Rheology thus shows that QRs at best only slightly improve the mechanical strength and stabilities of the hybrid gels as compared to the pristine gel, but at the same time do not disrupt the networks. The marginal improvement of the mechanical strength and thermal stability of the hybrid gels indicates the presence of *weak* non-covalent interactions between the QRs and DEALI nanofibers.

2.3. Imaging of the DEALI-QR Hybrid Material

TEM imaging was performed in order to further investigate the interaction between QRs and the nanofibers (NFs) of the organogel. The self-aggregation tendency of the QRs is broken by the NFs leading to the assembly of mostly individual QRs on the gel network, as shown schematically in Figure 4a. The dispersion of 500 nM QRs ($L = 20 \pm 1$ nm, $D = 5.7 \pm 1$ nm) in the gel does not disrupt the gel network, as evidenced from Figure 4b. The QRs appear as bound to the gel nanofibers, although the images cannot clarify whether the QRs are within the fibers or on the surface (or both). Interestingly, some of the QRs were found to align on the surface of DEALI fibers, although majority of the QRs preferred to stay dispersed and did not align (Figure 4c–g). Furthermore, some of the QRs were presumably shorter or presented hexagonal (circular) faces due to the possible vertical orientation inside the fibers in the xerogel.

The alignment of QRs as linear arrays was clearly seen in Figure 4c and corresponding zoomed-in image in Figure 4d of the rectangular region. Similarly, several linear arrays with 23 QRs were seen in Figure 4e and the regions are zoomed-in (Figure 4f–g). Here again, it is interesting to notice that some QRs are vertically oriented in the NF (Figure 4g). To shed some

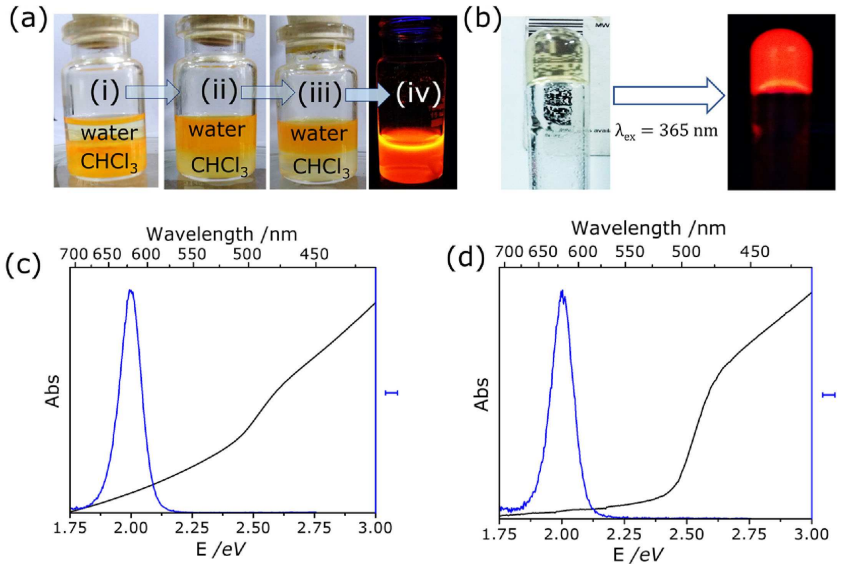

Figure 5. (a) Transfer of CdSe-CdS QRs (S-in-R) from organic to aqueous phase (i–iii); highly red luminescent CdSe-CdS QRs in water under UV-light (λ_{ex} = 365 nm, iv); (b) photograph of CaCh (10/20 mM) hydrogel with CdSe-CdS QRs (S-in-R, 50 nM) under ambient and UV-light (λ_{ex} = 365 nm); absorption (black) and PL (blue, excitation wavelength = 425 nm) spectra of (c) TGA-capped QRs (50 nM) in water and (d) TGA-capped QRs (50 nM) in CaCh hydrogel (10/20 mM).

light into this kind of differential dispersion of QRs with some of them appearing as linear arrays in the hybrid and others staying mostly as single individuals, we can point out the solubility criteria of the QRs. Since the QRs solubilize well in DCB, the individual particles are more likely to be trapped by the 3D network of fibers during gelation rather than forming assemblies (as seen when the solvent is evaporated in absence of gel). This is coherent with previous report from our group.[44] In this case, the alignment of QRs appears to require an increase of their local concentration such that the QRs can be in contact at their ends. However, the efficient dispersion opposes to this phenomenon.

2.4. Hybrid Material of CdSe-CdS QRs (S-in-R) and CaCh Hydrogel

In order to provoke a drastic change of the QRs environment, water was chosen as a solvent for a different hybrid material. This requires using a different gelator, although of the same family as in the previous case (Figure S1). CdSe-CdS QRs (S-in-R, 65 nm long) were dispersed in water with a hydrogelator derived from bile acid, calcium cholate (CaCh). The QRs require a different ligand to be at least partially dispersible in water. Therefore, TOPO was exchanged with thioglycolic acid (TGA) using a biphasic method, additionally negatively charging the ligands by deprotonation of TGA with a base (ethylenediamine). The TGA capped CdSe-CdS QRs (50 nM) show red-shifted emission (~6 nm) as compared to the original QRs in hexane, possibly owing to hydrophobicity-driven aggregation of the QRs in water (Figure 5c).[70] The luminescence quantum yield of the particles decreases to 15% (Figure 5).[71] In the hybrid hydrogel (Ca^{2+} : NaCh = 10 mM : 20 mM), the emission maximum of the QRs remains at the same wavelength, whereas the absorption spectra becomes featureless in the lower energy region (Figure 5d).

Insight into the stability of the Ca–Ch/QR hybrid materials was obtained by dynamic rheology experiments. Dynamic frequency sweep experiment of pristine Ca–Ch gel (10/20 mM) and Ca–Ch gel containing 50 nM QRs reveal that the shear storage modulus (G') for the hybrid gel is around 17.3 kPa (at frequency 1 Hz), which is of the same order as the pristine CaCh gel (19.8 kPa, Figure S8). The ratio of G'/G'' (4.9–5.5) were also typical for viscoelastic gels. The yield stress (σ^*) value of the hybrid gel was marginally higher than the pristine CaCh hydrogel. Overall, the rheology experiments suggest that the mechanical and flow properties of Ca–Ch hydrogels were not significantly altered by doping with QRs at the concentration used (Table S1).

2.5. Imaging of CaCh-QR Hybrid Materials

Imaging of the hybrid hydrogel with TEM (Figure 6) revealed a very interesting behaviour of the QRs. Indeed, elongated wire-like structures are formed by end-to-end self-assembly of QRs (Figure 6a–e). Elongated QR-chains, in some cases reaching lengths >150 nm, form in the hydrophobic domain of the hydrogel fibres. The QRs interact through their tips forming linear inter-connected chains, but can also present turns in the connection points of the QRs.[72] This is revealed by the HRTEM image in Figure 6f (red circles), showing the orientation of the facets of the QRs. The lattice planes with interplanar spacings of 0.35 and 0.33 nm are clearly visible and correspond to (002)

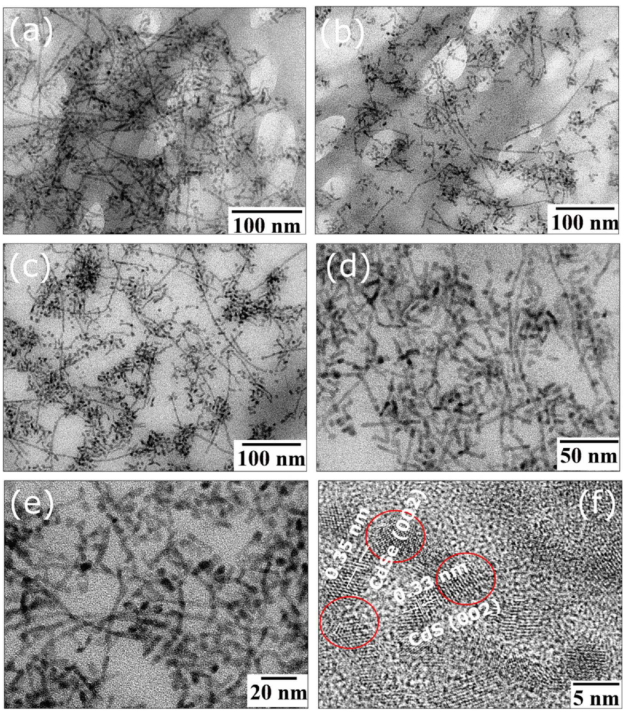

Figure 6. 50 nM CdSe-CdS QRs (S-in-R) in 10/20 mM CaCh hydrogel: (a–e) TEM images of different regions at different magnification; (f) HRTEM image showing linked QRs through their tips and lattice planes.

planes of CdSe and CdS lattices of the QRs, showing different orientations due to the relative angles occurring at the tips' connection. It can be noted in these images that QRs can appear shorter than their original length. This could be due to an out-of-plane orientation within the gel deposit on the TEM grid or due to some truncation or erosion occurring during the processing of the QRs into the hybrid material.[73] However, contrasting with this interpretation, no luminescence "pollution" by CdS shell residuals is observed. Thus, the hydrogels fibres provide a hydrophobic environment where the TGA-capped QRs are driven to connect to each other in a particular way due to their amphiphilicity (Figure 7a).

The mechanism by which the QRs connect with each other in the hydrogel can be proposed to be based on the preferential desorption of bifunctional thiolate ligands TGA on the tips of the QRs (Figure 7b). Since it was shown previously that thiol binds more strongly to the Cd^{2+} atoms on the sides of the QR as compared to the tips of the QRs, the ligands are thought to be more weakly-bound at these ends.[9,71] Therefore, the electrostatic repulsion between the negatively charged carboxylate moieties of the TGA could lead to the desorption of the ligand preferentially from the tips of the QRs, rendering them locally more hydrophobic. Since the negatively charged carboxylate moieties procure a more hydrophilic nature to the sides of the QRs, the hydrophobic ends of the amphiphilic QRs may tend to associate more tightly while the sides repel each other. After the end-to-end-assembly, the QRs bind more extensively leading to entanglement and nanowire formation, whereas some shorter QRs dissociate as broken-off parts from the wires. The gel 3D SAFIN network provides a hydrophobic scaffold on which these connected QRs can be stabilized and dispersed (Figure 7c).[54] These elongated wire formation assisted by hydrophobic nanofibers have not been reported yet in literature.

3. Summary and Conclusion

A robust methodology was developed to synthesize core-shell CdSe-CdS QRs (S-in-R and R-in-R) with varying length and diameters and different shapes of the core with a highly thermally stable steroidal precursor: $Cd(DCh)_2$. The QRs were highly luminescent (QY: 40–75%) and showed high crystallinity and size-homogeneity. The S-in-R QRs were shown to be dispersible on organogel fibres of DEALI in DCB, or in hydrogels of CaCh, at the condition that the QRs were capped with appropriate ligands conveying a sufficient dispersibility in the solvent (TOPO in the case of an organic solvent and TGA in water). This yields macroscopically homogeneous, stable, translucent and luminescent hybrid gels. In addition, arrays of oriented quantum rods are found to form into or onto gel nanofibers. This orientation occurs by a tip-to-tip interaction and QR-chain formation. The NFs provide a scaffold that stabilizes the linear QR assemblies. It was shown that QRs can be driven to form this type of interaction by using negatively charged capping ligands that induce a certain degree of amphiphilicity by partial unbinding on tip-ends, in the particular solvent that is water. The combination of nanofiber-forming hydrogelators and elongated quantum rods is promising in the perspective to form hybrid nanostructures with anisotropic optic or electronic properties.

Experimental Section

Materials

Trioctylphosphine (97%), trioctylphosphine oxide (99%), cadmium nitrate tetrahydrate, sodium deoxycholate, Se powder, octadecylphosphonic acid (97%), tetradecylphosphonic acid (97%), hexylphosphonic acid (95%), ethylenediamine, 1,2-dichlorobenzene were purchased from Sigma-Aldrich, Fluka and local suppliers. Methanol, acetone, anhydrous hexane, ethanol and chloroform were purchased from Sigma-Aldrich. Fluorescence reference dyes coumarin 153 and rhodamine 101 were purchased from Sigma-Aldrich and Exciton.

Synthesis of Cadmium Deoxycholate

Cadmium deoxycholate ($Cd(DCh)_2$) precursor was prepared at a large scale using a previously reported procedure.[59] Thus, Cd $(NO_3)_2$, $4H_2O$ and sodium deoxycholate were mixed together in methanol at room temperature to obtain a white gelatinous precipitate, which was isolated by filtration and dried subsequently.

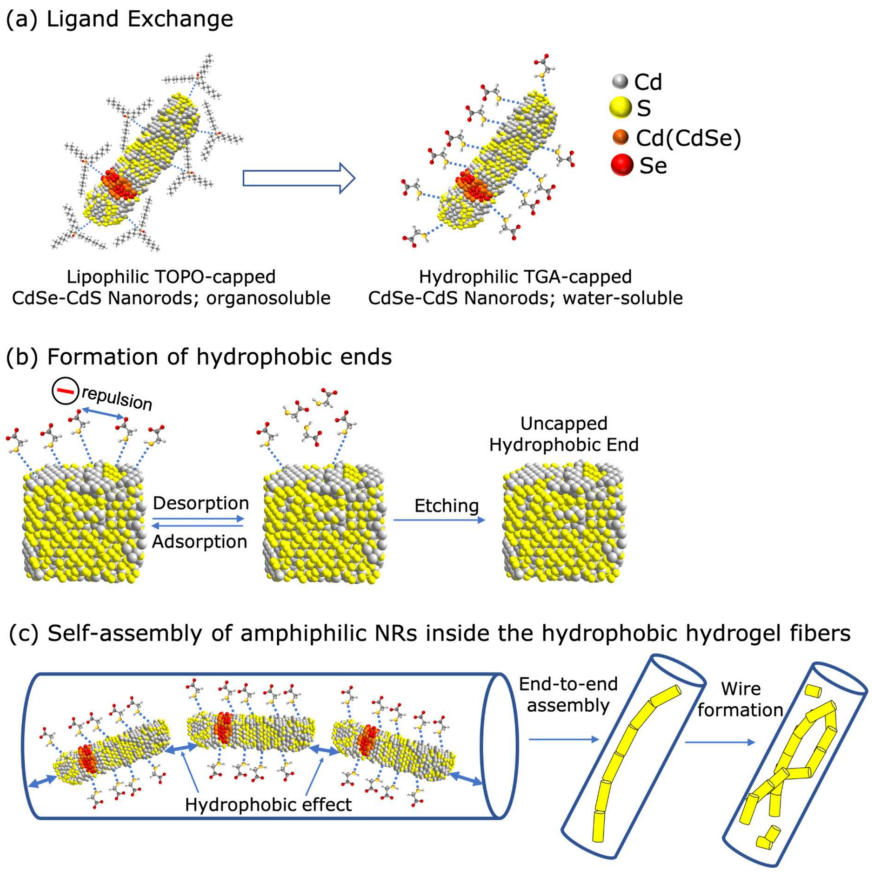

Figure 7. Schematic showing QR-NF interactions in the hydrogel: (a) ligand exchange of TOPO with TGA rendering the QRs water-soluble; (b) hydrophobic ends of QRs formed due differential adsorption-desorption of thiocarboxylate ligands; (c) chain formation through end-to-end linking of the QRs on the hydrophobic regions of the SAFIN.

Synthesis of Spherical Wurtzite Seeds

The spherical wurtzite CdSe seeds were prepared following a previously reported procedure using cadmium deoxycholate as Cd precursor.[44]

Synthesis of CdSe Rod Seeds

Se (11 mg, 0.14 mmol) was dissolved in 1.2 mL TOP by heating at 80 °C for 10 min and subsequently was cooled to room temperature with degassing. In a 3-necked round-bottomed flask, TOPO (2 g), octadecylphosphonic acid (150 mg), tetradecylphosphonic acid (20 mg) and hexylphosphonic acid (50 mg) were mixed with Cd $(DCh)_2$ (250 mg, 0.28 mmol) and heated at a rate of 15 °C/min to 340 °C. At this point, 1 mL TOP was quickly injected, and the temperature dropped to 310 °C. Temperature was allowed to reach to 340 °C and 1.2 mL TOPSe was rapidly injected. Temperature was set to 290 °C and run for 10 min. After that the reaction was stopped to obtain red emitting wurtzite CdSe QRs and quenched with 10 mL of hexane. To purify CdSe QRs, 3 mL of QRs solution was precipitated with 25 mL acetone-methanol (4:1) and centrifuged at 7000 rpm for 15 min and the isolated precipitate was washed with acetone-methanol 3–4 times and finally it was dispersed in hexane (1 mL).

Synthesis of CdSe-CdS QRs (Sphere in rod, S-in-R)

CdSe-CdS QRs (S-in-R) were prepared following a previously reported procedure using cadmium deoxycholate as Cd precursor.[44]

Synthesis of CdSe-CdS QRs (rod in rod, R-in-R)

Wurtzite CdSe rods dissolved in 1 mL hexane was evaporated and re-dissolved in 0.5 mL TOP (conc. 200–300 μM) upon heating and sonication. Sulfur powder (45 mg, 1.4 mmol) was dissolved in 0.5 mL TOP by heating at 90 °C for 15 min. The seed solution and sulfur solution were mixed with each other and degassed at room temperature. In a 3-necked round-bottomed flask, TOPO (2 g), ODPA (180 mg), HPA (50 mg), TDPA (20 mg), $Cd(DCh)_2$ (255 mg, 0.28 mmol) were mixed together under Ar and heated to 340 °C at a rate of 20 °C/min. At this temperature, 1 mL TOP was rapidly injected, and temperature dropped to 305 °C and it was allowed to reach to 340 °C. Then 1 mL of w-CdSe rods/TOPS was quickly injected. The temperature was set at 320 °C and run for 7 min. After that, the reaction was stopped by removing the heating mantle and diluting with hexane. The CdSe-CdS QRs (R-in-R) were purified by precipitation using acetone as the non-solvent with centrifugation speed of 7000 rpm for 10 minutes. The purified precipitate was collected and dispersed in hexane.

Ligand Exchange and Water-Solubilization of QRs (S-in-R)

The QRs (2 mg) in hexane was precipitated with acetone and centrifuged and washed with acetone another 2–3 times. The purified QRs were then dispersed in 5 mL $CHCl_3$ followed by addition of ethylenediamine (0.2 mL). The solution was stirred in a vial and an aqueous suspension of thioglycolic acid (0.1 mL in 5 mL water) was added to clearly observe the two phases. The biphasic mixture was stirred vigorously at room temperature for 2 h to completely transfer the hydrophobic QRs to the aqueous phase. Ethanol was added to precipitate and isolate the QRs by centrifugation. Finally, the purified and ligand exchanged QRs were dispersed in 5 mL water by mild sonication to obtain optically translucent stable aqueous solutions of QRs for further studies.

Preparation of Hybrid Materials

The organogel-QR hybrid material was prepared by dissolving known amount of the originally TOPO-capped QRs in the gelating solvent DCB containing the gelator. The resulting mixture was heated at 90 °C for 5 min and then cooled to room temperature to obtain a yellow-brown translucent hybrid organogel. In case of the hydrogel, the TGA capped QRs were mixed with aqueous sodium cholate and heated at 55 °C for 5 min. Similarly, aqueous $Ca(NO_3)_2$ solution was heated at 55 °C for 5 min and mixed together to form a yellow-brown translucent hybrid hydrogel.

Characterization Techniques

Absorption and Emission Measurements

The as-prepared CdSe spherical QDs were dispersed in chloroform and rod seeds, CdSe-CdS QRs dispersions were diluted with hexane to prepare the solutions for absorption and photoluminescence (PL) studies. Absorption spectra were recorded using a Varian Cary 5000 UV-Vis NIR spectrophotometer and PL spectra were recorded using a Horiba Scientific Fluoromax-4 Spectrofluorometer. For PL quantum yield (QY) measurements, the absorbance of the CdSe-CdS QRs and the reference dye were adjusted so that they were comparable ($A < 0.1$). Photoluminescence of the QRs and dye samples were recorded using the same excitation wavelengths, but owing to the small Stokes shift in QRs, the excitation had to be performed at $\lambda_{ex} < \lambda_{max}$ of absorption. The integrated area under the PL curve was calculated giving the PL QY value using standard equations.[74]

Electron Microscopy

The purified CdSe-CdS QRs (S-in-R, R-in-R) were dispersed in hexane and dilute solutions (7–8 μL) of the samples were drop-casted over the carbon-coated copper grids and dried before the experiment. For the preparation of gel-QR hybrid sample, the TEM grid was touched with a thin layer of gel and excess sample was removed by gently pressing on a tissue paper. HRTEM images and Energy Dispersive X-ray Spectroscopy (EDS) pattern were collected with a JEOL 2200 FS and JEOL JEM-2100F microscope, operating at 200 kV with a field emission gun and point resolution of 0.23 nm.

Rheology

The rheological studies of the gels were carried out using a Stress-Controlled AR1000 (TA Instruments) rheometer. A serrated rotor with parallel plate cross-hatched geometry (d, 20 mm) was utilized in all these measurements. The temperature of the plate was controlled at 25 °C (±0.1 °C). In case of the organogel, a hot sol (~ 90 °C) was put carefully on the plate and kept for 3 min under the cover for gel formation. On the other hand, warm calcium nitrate and sodium cholate aqueous solutions (~55 °C) were mixed together to form a hybrid hydrogel which was scooped up and transferred to the rheometer plate. The rotor was then brought down to 500 μm geometry gap by slowly pressing the gel. The excess sample was trimmed and taken off, and the experimental gap was set to 400 μm stabilizing the gel for another 1 h. To prevent the evaporation of the solvent, additional precautions were taken.

T_{gel} Tests

The thermal stability of the hybrid organo/hydrogel and pristine gels was determined by "inverted test tube" method. In this method, sealed Pyrex tubes containing the gels were kept inverted in a water bath and heated at a rate of 2 °C/min. The temperatures at which the gels fell under gravity, was noted down as the T_{gel}.

Supporting Information

Additional experimental data, FTIR, XRD of CdSe QDs and CdSe-CdS QRs, additional TEM images are included as Supporting Information. The Supporting Information is available free of charge on the Wiley Online Library.

Acknowledgements

The project was financially supported by CEFIPRA (project 4805-1), the CNRS, the French Ministry of Education and Research and Région Aquitaine. We thank Ms S. Buffière, PLACAMAT and Chemical Sciences Division at IISc Bangalore for recording TEM images.

Conflict of Interest

The authors declare no conflict of interest.

Keywords: hydrogels · nanowires · organogels · quantum rods · self-assembly

[1] H. Li, A. G. Kanaras, L. Manna, *Acc. Chem. Res.* **2013**, *46*, 1387.
[2] L. Manna, E. Scher, A. P. Alivisatos, *J. Am. Chem. Soc.* **2000**, *122*, 12700.
[3] P. Reiss, M. Carrière, C. Lincheneau, L. Vaure, S. Tamang, *Chem. Rev.* **2016**, *116*, 10731.
[4] J. Chang, E. R. Waclawik, *RSC Adv.* **2014**, *4*, 23505.
[5] P. Reiss, M. Protière, L. Li, *Small* **2009**, *5*, 154.
[6] N. A. Kotov, *Science* **2010**, *330*, 188.
[7] N. A. Kotov, P. S. Weiss, *ACS Nano* **2014**, *8*, 3101.
[8] Z. Nie, A. Petukhova, E. Kumacheva, *Nat. Nanotechnol.* **2010**, *5*, 15.
[9] Y. Taniguchi, T. Takishita, T. Kawai, T. Nakashima, *Angew. Chem. Int. Ed.* **2016**, *55*, 2083.
[10] J. Hu, L. Li Ls, W. Yang, L. Manna, L. Wang Lw, A. P. Alivisatos, *Science* **2001**, *292*, 2060.
[11] I. Hadar, G. B. Hitin, A. Sitt, A. Faust, U. Banin, *J. Phys. Chem. Lett.* **2013**, *4*, 502.

[12] E. Rothenberg, Y. Ebenstein, M. Kazes, U. Banin, *J. Phys. Chem. B* **2004**, *108*, 2797.
[13] A. R. Dhawan, F. Feng, L. Coolen, A. Maître, *IEEE Photonics J.* **2015**, *7*, 1.
[14] I. Coropceanu, A. Rossinelli, J. R. Caram, F. S. Freyria, M. G. Bawendi, *ACS Nano* **2016**, *10*, 3295.
[15] L. Carbone, C. Nobile, M. De Giorgi, F. Della Sala, G. Morello, P. Pompa, M. Hytch, E. Snoeck, A. Fiore, I. R. Franchini, M. Nadasan, A. F. Silvestre, L. Chiodo, S. Kudera, R. Cingolani, R. Krahne, L. Manna, *Nano Lett.* **2007**, *7*, 2942.
[16] D. V Talapin, J. H. Nelson, E. V Shevchenko, S. Aloni, B. Sadtler, A. P. Alivisatos, *Nano Lett.* **2007**, *7*, 2951.
[17] A. Sitt, A. Salant, G. Menagen, U. Banin, *Nano Lett.* **2011**, *11*, 2054.
[18] H. Eshet, M. Grünwald, E. Rabani, *Nano Lett.* **2013**, *13*, 5880.
[19] Y. Jang, A. Shapiro, M. Isarov, A. Rubin-Brusilovski, A. Safran, A. K. Budniak, F. Horani, J. Dehnel, A. Sashchiuk, E. Lifshitz, *Chem. Commun.* **2017**, *53*, 1002.
[20] C. She, A. Demortière, E. V. Shevchenko, M. Pelton, *J. Phys. Chem. Lett.* **2011**, *2*, 1469.
[21] J. Muller, J. M. Lupton, P. G. Lagoudakis, F. Schindler, R. Koeppe, A. L. Rogach, J. Feldmann, D. V. Talapin, H. Weller, *Nano Lett.* **2005**, *5*, 2043.
[22] A. Sitt, F. Della Sala, G. Menagen, U. Banin, *Nano Lett.* **2009**, *9*, 3470.
[23] D. Steiner, D. Dorfs, U. Banin, F. D. Sala, L. Manna, O. Millo, *Nano Lett.* **2008**, *8*, 2954.
[24] M. Zanella, G. Bertoni, I. R. Franchini, R. Brescia, D. Baranov, L. Manna, *Chem. Commun.* **2011**, *47*, 203.
[25] D. Baranov, A. Fiore, M. Van Huis, C. Giannini, A. Falqui, U. Lafont, H. Zandbergen, M. Zanella, R. Cingolani, L. Manna, *Nano Lett.* **2010**, *10*, 743.
[26] C. Nobile, L. Carbone, A. Fiore, R. Cingolani, L. Manna, R. Krahne, *J. Phys. Condens. Matter* **2009**, *21*, 1.
[27] F. Pietra, F. T. Rabouw, P. G. Van Rhee, J. Van Rijssel, A. V Petukhov, B. H. Erné, P. C. M. Christianen, C. De Mello Donegá, D. Vanmaekelbergh, *ACS Nano* **2014**, *8*, 10486.
[28] N. Gaponik, A. K. Herrmann, A. Eychmüller, *J. Phys. Chem. Lett.* **2012**, *3*, 8.
[29] H. Chen, V. Lesnyak, N. C. Bigall, N. Gaponik, A. Eychmüller, *Chem. Mater.* **2010**, *22*, 2309.
[30] V. Sayevich, B. Cai, A. Benad, D. Haubold, L. Sonntag, N. Gaponik, V. Lesnyak, A. Eychmüller, *Angew. Chem. Int. Ed.* **2016**, *55*, 6334.
[31] S. Naskar, A. Freytag, J. Deutsch, N. Wendt, P. Behrens, A. Köckritz, N. C. Bigall, *Chem. Mater.* **2017**, *29*, 9208.
[32] S. Naskar, J. F. Miethe, S. Sánchez-Paradinas, N. Schmidt, K. Kanthasamy, P. Behrens, H. Pfnür, N. C. Bigall, *Chem. Mater.* **2016**, *28*, 2089.
[33] I. U. Arachchige, S. L. Brock, *J. Am. Chem. Soc.* **2006**, *128*, 7964.
[34] J. L. Mohanan, I. U. Arachchige, S. L. Brock, *Science* **2005**, *307*, 397.
[35] Z. Tang, N. A. Kotov, *Adv. Mater.* **2005**, *17*, 951.
[36] M. Grzelczak, J. Vermant, E. M. Furst, L. M. Liz-Marzán, *ACS Nano* **2010**, *4*, 3591.
[37] D. V Talapin, E. V Shevchenko, C. B. Murray, A. Kornowski, S. Föraster, H. Weller, *J. Am. Chem. Soc.* **2004**, *126*, 12984.
[38] S. Sánchez-Paradinas, D. Dorfs, S. Friebe, A. Freytag, A. Wolf, N. C. Bigall, *Adv. Mater.* **2015**, *27*, 6152.
[39] T. Mokari, E. Rothenberg, I. Popov, R. Costi, U. Banin, *Science* **2004**, *304*, 1787.
[40] P. S. Shah, M. B. Sigman, C. A. Stowell, K. T. Lim, K. P. Johnston, B. A. Korgel, *Adv. Mater.* **2003**, *15*, 971.
[41] J. He, Q. Zhang, S. Gupta, T. Emrick, T. P. Russell, P. Thiyagarajan, *Small* **2007**, *3*, 1214.
[42] J. L. Baker, A. Widmer-Cooper, M. F. Toney, P. L. Geissler, A. P. Alivisatos, *Nano Lett.* **2010**, *10*, 195.
[43] N. Zhao, K. Liu, J. Greener, Z. Nie, E. Kumacheva, *Nano Lett.* **2009**, *9*, 3077.
[44] A. Chakrabarty, G. Raffy, M. Maity, L. Gartzia-Rivero, S. Marre, C. Aymonier, U. Maitra, A. Del Guerzo, *Small* **2018**, *14*, 1802311.
[45] D. Kritchevsky, P. P. Nair, *Bile Acids Chem. Physiol. Metab.*, Springer US, Boston, MA, **1971**, pp. 1–10.
[46] H. L. J. Makin, *Gut* **1986**, *27*, 1232.
[47] S. Mukhopadhyay, U. Maitra, *Curr. Sci.* **2004**, *87*, 1666.
[48] Nonappa, U. Maitra, *Soft Matter* **2007**, *3*, 1428.
[49] Y. Hishikawa, K. Sada, R. Watanabe, M. Miyata, K. Hanabusa, *Chem. Lett.* **2003**, *27*, 795.
[50] K. Nakano, Y. Hishikawa, K. Sada, M. Miyata, K. Hanabusa, *Chem. Lett.* **2005**, *29*, 1170.
[51] H. M. Willemen, T. Vermonden, A. T. M. Marcelis, E. J. R. Sudhölter, *Eur. J. Org. Chem.* **2001**, *2001*, 2329.
[52] H. M. Willemen, A. T. M. Marcelis, E. J. R. Sudhölter, W. G. Bouwman, B. Demé, P. Terech, *Langmuir* **2004**, *20*, 2075.
[53] H. M. Willemen, T. Vermonden, A. T. M. Marcelis, E. J. R. Sudhölter, *Langmuir* **2002**, *18*, 7102.
[54] A. Chakrabarty, U. Maitra, A. D. Das, *J. Mater. Chem.* **2012**, *22*, 18268.
[55] U. Maitra, S. Mukhopadhyay, A. Sarkar, P. Rao, S. S. Indi, *Angew. Chem. Int. Ed.* **2001**, *40*, 2281.
[56] S. Bhowmik, S. Banerjee, U. Maitra, *Chem. Commun.* **2010**, *46*, 8642.
[57] S. Banerjee, R. Kandanelli, S. Bhowmik, U. Maitra, *Soft Matter* **2011**, *7*, 8207.
[58] U. Maitra, A. Chakrabarty, *Beilstein J. Org. Chem.* **2011**, *7*, 304.
[59] A. Chakrabarty, S. Chatterjee, U. Maitra, *J. Mater. Chem. C* **2013**, *1*, 2136.
[60] Y. A. Yang, H. Wu, K. R. Williams, Y. C. Cao, *Angew. Chem. Int. Ed.* **2005**, *44*, 6712.
[61] L. A. Swafford, L. A. Weigand, M. J. Bowers, J. R. McBride, J. L. Rapaport, T. L. Watt, S. K. Dixit, L. C. Feldman, S. J. Rosenthal, *J. Am. Chem. Soc.* **2006**, *128*, 12299.
[62] P. D. Wadhavane, R. E. Galian, M. A. Izquierdo, J. Aguilera-Sigalat, F. Galindo, L. Schmidt, M. I. Burguete, J. Pérez-Prieto, S. V. Luis, *J. Am. Chem. Soc.* **2012**, *134*, 20554.
[63] S. Bhat, U. Maitra, *Chem. Mater.* **2006**, *18*, 4224.
[64] S. Chatterjee, B. Kuppan, U. Maitra, *Dalton Trans.* **2018**, *47*, 2522.
[65] R. K. Das, S. Bhat, S. Banerjee, C. Aymonier, A. Loppinet-Serani, P. Terech, U. Maitra, G. Raffy, J. P. Desvergne, A. Del Guerzo, *J. Mater. Chem.* **2011**, *21*, 2740.
[66] N. M. Sangeetha, S. Bhat, A. R. Choudhury, U. Maitra, P. Terech, *J. Phys. Chem. B* **2004**, *108*, 16056.
[67] P. Terech, N. M. Sangeetha, U. Maitra, *J. Phys. Chem. B* **2006**, *110*, 15224.
[68] H. Wu, M. Morbidelli, *Langmuir* **2001**, *17*, 1030.
[69] W. H. Shih, W. Y. Shih, S. Il Kim, J. Liu, I. A. Aksay, *Phys. Rev. A* **1990**, *42*, 4772.
[70] R. Calzada, C. M. Thompson, D. E. Westmoreland, K. Edme, E. A. Weiss, *Chem. Mater.* **2016**, *28*, 6716.
[71] M. Q. Dai, L. Y. L. Yung, *Chem. Mater.* **2013**, *25*, 2193.
[72] A. Figuerola, I. R. Franchini, A. Fiore, R. Mastria, A. Falqui, G. Bertoni, S. Bals, G. Van Tendeloo, S. Kudera, R. Cingolani, L. Manna, *Adv. Mater.* **2009**, *21*, 550.
[73] B. P. Khanal, E. R. Zubarev, *ACS Nano* **2019**, *13*, 2370.
[74] M. Grabolle, M. Spieles, V. Lesnyak, N. Gaponik, A. Eychmüller, U. Resch-Genger, *Anal. Chem.* **2009**, *81*, 6285.

Manuscript received: July 18, 2019
Revised manuscript received: August 21, 2019
Accepted manuscript online: August 27, 2019
Version of record online: September 16, 2019